Inconsistent phenomenon of thermoelectric load resistance for photovoltaic–thermoelectric module

Guiqiang Li[a, b, *]

ligq@mail.ustc.edu.cn

Kai Zhou[a]

Zhiying Song[a]

Xudong Zhao[b, *]

Xudong.zhao@hull.ac.uk

Jie Ji[a]

[a]Department of Thermal Science and Energy Engineering, University of Science and Technology of China, 96 Jinzhai Road, Hefei City 230026, China

[b]School of Engineering, University of Hull, Hull HU6 7RX, UK

*Corresponding authors at: Department of Thermal Science and Energy Engineering, University of Science and Technology of China, 96 Jinzhai Road, Hefei City 230026, China (G. Li).

Abstract

Combing PV with Thermoelectric (TE) would be dominant because it can employ the solar fully spectrum to produce electricity. But the TE efficiency is significantly lower than PV efficiency and the coupling effect between them will limit the performance of PV and TE. The analyze and comparison on the different characteristics among the hybrid module, the PV alone and TE alone is significant to obtain the highest the electrical efficiency. In this paper, the attention was paid to the inconsistent phenomenon of thermoelectric load resistance for photovoltaic–thermoelectric modules. The model of PV-TE was built and verified based on two types of PV cells. The load resistance of TE for the maximum power output was also analyzed under different working conditions for the TE alone, TE in the PV-TE and PV-TE. The results showed that the load resistance of TE for the maximum power output of the TE alone, TE in the PV-TE and PV-TE are all different. For example, the PV-TE module based on the c-Si cell attains its peak value at the load electrical resistance of TE of 0.75 Ω, while the internal electrical resistance of the TE is 0.47 Ω. The PV-TE module based on the GaAs cell shows a maximum efficiency of PV-TE with a load resistance of approximately 1.6 Ω, while the internal electrical resistance of the TE is 2.0 Ω. Referring to the load resistance of TE alone is not suitable for PV-TE maximum power output. In addition, the TE maximum power output does not correspond to the PV-TE maximum power output since the TE load resistances in these two conditions are also different. The study will provide the reference for attaining the correct load resistance for the actual maximum power output of PV-TE module.

Keywords: Migration; Load resistance; Maximum power output; PV-TE

Nomenclature

A

area of PV (m^2)

C

concentration ratio

C_p

specific heat of air (KJ/(kg K))

E_{pv}

power of the solar cell (W)

E_{in}

incident solar energy (W)

G

solar radiation (W/m^2)

h_{rad}

coefficient of radiation heat transfer (W/(m^2 K))

h_{wind}

coefficient of radiation heat transfer (W/(m^2 K))

H

height of heat sink (m)

I

current (A)

K

total thermal conductance of a TE module (W/K)

K_{fin}

thermal conductivity of the fin (W/K)

L

length of the heat sink (m)

P_{teg}

power of the load resistance (W)

Pr

Prandtl number

Q_{flow}

energy that flowed from solar cell to hot side of the TEG

Q_h

energy that passed in hot side of the TEG (W)

Q_l

energy that passed in cold side of the TEG (W)

R_{conv}

thermal resistance of convection heat transfer between heat sink and ambient air (K/W)

R_{conf}

thermal resistance of the heat conduction in heat sink(K/W)

R_{fin}

thermal resistance of the heat sink (K/W)

R_{ct1}

thermal contactresistance between solar cell and TEG (K/W)

R_{ct2}

thermal contactresistance between heat sink and TEG (K/W)

R_{TE}

electric resistance of TE (Ω)

S_1

cross section area of the heat sink (m^2)

S_2

total area of the fin (m^2)

T_a

temperature of ambient air (K)

T_c

temperature of PV (K)

T_h

temperature of the hot side of TEG (K)

T_l

temperature of the cold side of TEG (K)

T_{sky}

temperature of sky (K)

u_f

wind speed (m/s)

α

Seeback coefficient (V/K)

σ

Stefan-Boltzmann constant (W/(m^2 K^4))

ε

emissivity of the PV

η_c

photoelectric efficiency at standard condition

ϕ_c

solar cell temperature coefficient

ρ

density of air (kg/m^3)

μ

kinematic viscosity (m^2/s)

1 Introduction

Photovoltaic (PV) is one of the most common and commercialized ways for electrical generation [1]. With the PV technology development, PV efficiency has been increased significantly, but it is still limited since the conventional materials can only effectively convert photons of energy close to the semiconductor band gap. Therefore, researchers are paying more attention on ways of utilizing a wider solar spectrum to produce more electricity.

Thermoelectric (TE) technology can directly convert heat into electricity due to the Seebeck effect. Similar to PV, it has the advantages of no noise, no pollution, no moving parts, etc. [2]. In fact, by contrast the solar energy that cannot be absorbed by PV will be converted into the heat and even negatively affect PV efficiency. Thus the combination the PV and TE may be a good way to produce more electricity based on the full solar spectrum. Van Sark analyzed the feasibility of hybrid PV-TE modules, and found the overall efficiency and annual energy yield would all increase [3]. Lamba and Kaushik built a model and indicated the performance of a concentrated PV-TE hybrid power generation system [4]. Wang et al. designed a novel PV–TE hybrid device employing the dye-sensitized solar cell (DSSC), which gave rise to an overall conversion efficiency larger than 13% [5].

However, it is also possible that the efficiency of the PV-TE is lower than that of the PV alone [6]. The higher temperature will increase the TE efficiency but decrease the PV efficiency, so the coupling relationship between the PV and TE is complex, which can affect the performance of PV and TE. Pang et al. studied the impacts of the heat sink for PV-TE [7]. Zhu et al. optimized the thermal management for the high-performance photovoltaic-thermoelectric hybrid power generation system [8]. Zhang and Chau proposed a PV–TE hybrid system for automobiles and optimized the power output with maximum power point tracking (MPPT) technique [9,10]. Zhang et al. described the integration of polymer solar cell and TE module for doubling energy harvesting and increasing the open-circuit voltage [11]. Park et al. simulated and tested a lossless hybrid design through matching the internal resistance of TE to convey photocurrents without sacrificing the PV fill factor, and results showed an increase of conversion efficiency by ~30% [12].

Generally speaking, for the TE alone, when the load electrical resistance equals to or is slightly higher than the internal electrical resistance, the maximum power output can be obtained [13–15]. However, for the hybrid PV-TE module, it may be different from the TE alone operation, and the optimized working temperature may not match the load resistance as the same as that with which the TE alone has the maximum power output, since the factors of PV efficiency and the effect each other need to be considered. In addition, for the PV-TE module, even if the load resistance matches the TE maximum power output, one may not match the PV-TE maximum power output, and the

inconsistent phenomenon of the TE load resistance may occur. Therefore, the verification of the inconsistent phenomenon and the analysis on it would be of befit for distinguishing the load resistances in different conditions, and for obtaining the actual PV-TE maximum power output. However, at present, there are few studies on the inconsistent phenomenon of the load resistances in the hybrid module.

Therefore, in this paper, the inconsistent phenomenon of TE load resistance for PV-TE maximum power output is introduced. The model of the PV-TE is built then the simulation outcome is verified and the migration phenomenon is indicated. In addition, based on two types of the PV cells, the migration phenomenon on different environmental conditions is also discussed. The paper also provides the reference on the load resistance optimization to obtain the higher efficiency for PV-TE application.

2 Mathematical model

2.1 PV-TE module description

The PV-TE module is shown in Fig. 1. The sunlight can be concentrated by the solar concentrator, then part of this energy will be absorbed by the PV. The excess energy can be converted into the heat to be transferred to the TE. This creates a temperature gradient across the TE module, thus resulting in a thermal to electrical conversion. At last, the remaining thermal energy will be dispatched to the heat sink.
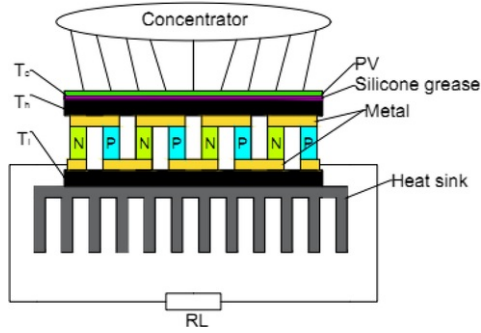
Fig. 1 Schematic diagram of the PV-TE module.

This study is intended to analyze the steady state performance of the PV-TE module, and the following assumptions are adopted to simplify the problem.

- The energy balance equations are all on the steady state conditions.

- The analysis is based on the one dimensional heat transfer.

- The solar flux distribution and temperature distribution on the PV top surface are uniform.

- The energy loss through around the side of the module is ignored.

- The internal electrical resistance of the TE is considered as an approximate constant [16–18].

2.2 Model

The energy transfer process of the PV-TE module is shown in Fig. 2. According to the energy balance, the energy balance equation of the PV can be expressed as below,

$$E_{in} = E_{pv} + h_{rad}A(T_c - T_{sky}) + h_{wind}A(T_c - T_a) + Q_{flow} \tag{1}$$

where E_{in} is the solar energy absorbed by the PV-TE module. E_{pv} is the PV electrical output. h_{rad} is the radiation heat transfer coefficient. h_{wind} is the convective heat transfer coefficient. Q_{flow} is the thermal energy transferred from the PV into TE.
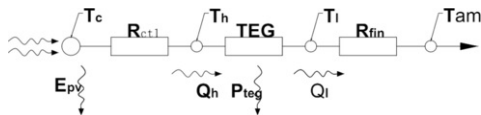
Fig. 2 Energy flow of the PV-TE module.

E_{in} can be expressed as

$$E_{in} = CGA\alpha_c \tag{2}$$

where C is the solar concentration ratio, and G is the solar radiation. A is the area of PV. α_c is the absorptivity of PV.

The electrical output is given by [19],

$$E_{pv} = CGA\alpha_c\eta_c \left[1 - \phi_c(T_c - 298)\right] \tag{3}$$

where η_c is the electrical efficiency at the standard condition. ϕ_c is the temperature coefficient.

h_{wind} can be defined as [20],

$$h_{wind} = 2.8 + 3u_w \tag{4}$$

where u_w is the wind speed.

h_{rad} can be defined as

$$h_{rad} = \varepsilon\sigma(T_c^2 + T_{sky}^2)(T_c + T_{sky}) \tag{5}$$

where ε is the emissivity of the PV. σ is Stefan-Boltzmann constant. T_c is temperature of the PV and T_a is the temperature of ambient air.

T_{sky} can be defined as

$$T_{sky} = 0.0552T_a^{1.5} \tag{6}$$

The energy flow from the PV to TE can be expressed as

$$Q_{flow} = \frac{T_c - T_h}{R_{ct1}}A \tag{7}$$

$$Q_{flow} = Q_h \tag{8}$$

where T_h is the hot side temperature of the TE. R_{ct1} is the thermal resistance between the PV and TE.

For the TE, the open circuit voltage V_{oc} can be given as

$$V_{oc} = \alpha(T_h - T_l) \tag{9}$$

where α is the Seebeck coefficient.

The electrical current can be obtained by

$$I = \frac{V_{oc}}{R_{TE} + R_L} \tag{10}$$

where R_{TE} is the internal electrical resistance. R_L is the load resistance.

Q_h and Q_l are the energy that passed in hot side and cold side of the TE respectively, which can be given as below [13],

$$Q_h = \alpha T_h I + K\Delta T - \frac{1}{2}I^2 R_{TE} \tag{11}$$

$$Q_l = \alpha T_l I + K\Delta T + \frac{1}{2}I^2 R_{TE} \tag{12}$$

where T_h and T_l are the temperature of the hot and cold sides respectively.

K is thermal conductivity of TE.

$$Q_l = \frac{T_l - T_a}{R_{fin}} \tag{13}$$

where R_{fin} is the thermal resistance between the TE and the ambient air.

$$R_{fin} = R_{ct2} + R_{conf} + R_{conv} \tag{14}$$

where R_{ct2} is the thermal contact resistance between the TE and the heat sink; R_{conf} is the resistance of the thermal conduction of the heat sink; R_{conv} is the thermal resistance between the heat sink and the ambient air.

R_{conf} can be expressed as

$$R_{conf} = \frac{H}{K_{fin} S_1} \tag{15}$$

where H is the height of the heat sink, K_{fin} is the thermal conductivity of the fin and S_1 is the cross section area of the heat sink.

In order to attain the value of R_{covf} which is the thermal resistance of convection heat transfer between fin and ambient air, the convection heat transfer coefficient h_{covf} can be obtained [21].

$$C_{fx} = 0.0592 Re_x^{-1/5} \tag{16}$$

$$Re_x = \frac{\rho u x}{\mu} \tag{17}$$

where u, ρ, μ represent velocity, density and viscosity coefficient of the fluid respectively. x is the characteristic length of the fin. $\rho = 1.1614$ $\mathrm{kg\,m^{-3}}$, $\mu = 1.846 * 10^{-5}$ $\mathrm{N\,s\,m^{-2}}$.

$$Nu_x = \frac{h_x x}{k_{air}} = 0.332 Re_x^{\frac{1}{2}} Pr^{\frac{1}{3}},\ 0.6 \leqslant Pr \leqslant 15 \tag{18}$$

$$Pr = \frac{\upsilon}{\alpha_1} = \frac{\mu C_p}{k_{air}} \tag{19}$$

where υ is the kinematic viscosity, h_x is the local heat transfer coefficient along the length of the fin, k_{air} is the thermal conductivity of air, C_p is the specific heat capacity of air, α_1 is the heat diffusivity. $\upsilon = 1.589 * 10^{-5}$ $\mathrm{m^2\,s^{-1}}$, $c_p = 1.007$ $\mathrm{kJ\,kg^{-1}\,K^{-1}}$, $\alpha_1 = 2.25 * 10^{-5}$ $\mathrm{m^2/s}$.

Thus St_x can be obtained as below,

$$St_x = \frac{Nu_x}{Re_x Pr} = \frac{h_x}{\rho C_p \mu_\infty} = 0.332 Re_x^{-1/2} Pr^{-2/3} \tag{20}$$

$$St_x Pr^{2/3} = C_{f,x}/2 \tag{21}$$

$$h_x = \frac{C_{f,x} \rho C_p u_\infty}{2 Pr^{2/3}} \tag{22}$$

And the local heat transfer coefficient h_x is obtained,

$$h_x = \frac{0.0296 x^{-1/5} \rho C_p \mu_\infty^{4/5}}{\upsilon^{-1/5} \cdot Pr^{2/3}} \tag{23}$$

Therefore,

$$h_{conv} = \frac{1}{L} \int_0^L h_x dx \tag{24}$$

After finishing calculated tablet on the air, the average heat transfer coefficient can be expressed as:

$$h_{\text{conv}} = \frac{0.037 L^{-1/5} \rho C_p u_\infty^{4/5}}{v^{-1/5} \cdot \text{Pr}^{2/3}}$$

(25)

Then the thermal resistance between the heat sink and the air is:

$$R_{conv} = \frac{v^{-1/5} \text{Pr}^{2/3}}{0.037 L^{-1/5} \rho C_p u_{hs}^{4/5} S_2}$$

(26)

where s_2 is the total area of the fin.

The TEG power output can be given by

$$P_{TE} = I^2 R_L$$

(27)

The efficiency of the TE can be expressed as

$$\eta_{te} = \frac{P_{te}}{Q_h}$$

(28)

So the total efficiency of the PV-TE can be expressed as below

$$\eta_{total} = \frac{E_{pv} + P_{te}}{CGA}$$

(29)

3 Theoretical model validation

In this paper, the two types of PV cells are introduced to verify the validity of the model, including c-Si and GaAs cells. The simulation parameters are shown in Table 1.

Table 1 Parameter detail of the simulation.

Parameter	Based on c-Si	Based on GaAs
Environment		
Solar radiation G	1000 W/m²	1000 W/m²
Prandtl number Pr	0.707	0.707
Ambient temperature T_a	298 K	298 K
Density of air ρ	1.1614 kg/m³	1.1614 kg/m³
Kinematic viscosity of air ν	$1.589 * 10^{-5}$ m²/s	$1.589 * 10^{-5}$ m²/s
Photovoltaic cells		
Area of PV A	40 * 40 mm²	6.4 * 6.4 mm²
Absorptivity of PV α_c	0.84	0.88
Emissivity of the PV ε	0.8	0.8

Efficiency at standard condition η_c	0.13	0.242
Solar cell temperature coefficient ϕ_c	0.0048/K	0.00275/K
TE		
Seebeck coefficient α	0.001 V/K	0.0077 V/K
Total thermal conductance of TEG K	0.0265 W/K	0.0132 W/K
The figure of merit Z	0.0085/K	0.0022/K
Thermal contact resistance between PV cell and TEG R_{ct1}	0.0009 K/(m² W)	0.00035 K/(m² W)
Thermal contact resistance between TEG and heat sink R_{ct2}	0.0001 K/W	0.0001 K/W
Heat sink		
Specific heat of air C_p	1007 J/(kg K)	1007 J/(kg K)
Height of heat sink H	0.005 m	0.0005 m
Thermal conductance of heat sink K_{fin}	230 W/(m K)	230 W/(m K)
Length of heat sink L	0.03 m	0.003 m
Internal resistance of TEG R_{TE}	0.44 Ω	2.0 Ω
Cross section area of the heat sink S_1	40 * 40 mm²	6.4 * 6.4 mm²
Total area of the fin S_2	0.019 m²	0.021 m²

The simulation and the verification were shown in Fig. 3. The total efficiency of the PV-TE and the TE efficiency with different load resistances are all compared, which indicates the well agreement.
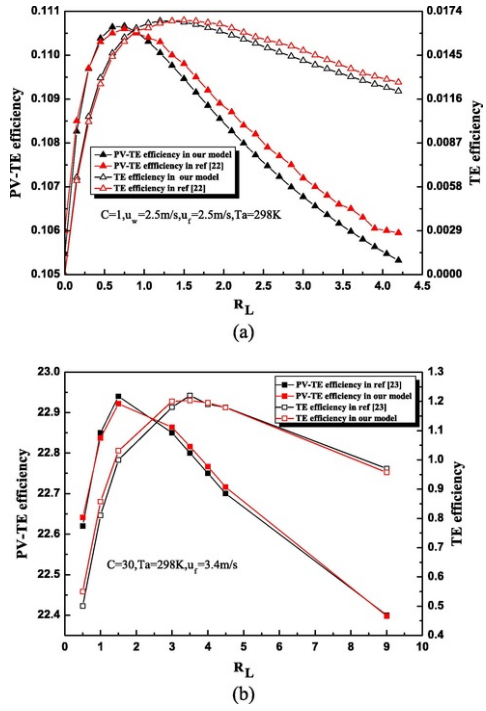
Fig. 3 The simulation and verification of the total efficiency and TE efficiency in PV-TE module (a) Based on c-Si cell (b) Based on GaAs cell.

According to Ref. [22], for the PV-TE module based on the c-Si cell, the internal electrical resistance of the TE is 0.47 Ω. But actually, when it is combined to PV, the TE maximum electrical output is corresponding to the load electrical resistance of about 1.40 Ω, while the PV-TE attains its peak value at the load electrical resistance of TE of 0.75 Ω. When the PV-TE module has the highest efficiency or the TE has the highest efficiency, the load electrical resistance has the different values, which present the inconsistent phenomenon and are all much larger than internal resistance of TE.

According to Ref. [23], for the PV-TE module based on the GaAs cell, the internal electrical resistance of the TE is 2.0 Ω. But for PV-TE module, the optimum load resistance for the TE maximum power generation is about 3.4 Ω, and the hybrid module shows a maximum efficiency of PV-TE with a load resistance of approximately 1.6 Ω. It is clear that whatever for the TE maximum power output in a PV-TE module or for the PV-TE maximum power output, the TE external load resistances are all different from the internal electrical resistance of TE, and the value of TE internal resistance is between that at the maximum power output of TE in the PV-TE module and that at the maximum power output of PV-TE module.

It also can be seen that for different types of PV cells, the migration phenomena of the TE load resistance for PV-TE module maximum power output all occur. These all may exist that the TE load resistance for PV-TE maximum power output is larger or lower than the TE internal resistance, even close to it at different working conditions. And the value of it is also different from that at the TE maximum power output for PV-TE module.

4 Result and discussion

4.1 PV-TE base on c-Si cell

When the ambient temperature is 298 K and the solar concentration ratio is one sun, the variation of the load resistances of TE is small (Fig. 4). With different wind speeds, the changes of the TE load resistances for PV-TE maximum power output and TE maximum power output are all small, but the TE load resistance for PV-TE maximum power output and the one for TE maximum power output in PV-TE are all larger than the internal electrical resistance of TE. When the wind speed is small, these values are all slightly higher than those with high wind speeds which may because of the low heat transfer performance on the cold side.
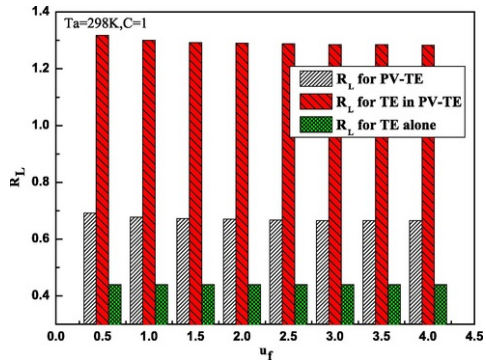
Fig. 4 Load resistances with different wind speeds (based on c-Si).

With the increase of the solar concentration ratio, the load resistance of the TE for PV-TE maximum power output has the similar values (Fig. 5). For the TE maximum power output in the PV-TE module, the load resistances of the TE presents a tendency to slowly rise. On the contrary, with the concentration ratio increases, the load resistance of the TE for the PV-TE maximum power output has a slight decrease tendency. But all of them are higher than the internal resistance of TE or load resistance of TE for TE alone significantly.
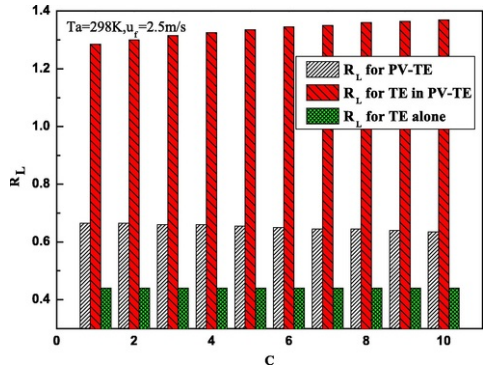
Fig. 5 Load resistances with different solar concentration ratios (based on c-Si).

It can be seen from Fig. 6 that the curve of the TE load resistance for TE maximum power output in PV-TE has a rising tendency when the environmental temperature increased, which is about 3 times than the internal resistance of TE. The value of the TE load resistance for PV-TE maximum is also approximately 1.5 times than the TE internal resistance. And the variation tendencies of the TE load resistance for PV-TE maximum output and for TE alone maximum output are not obvious with the environmental temperature increase.
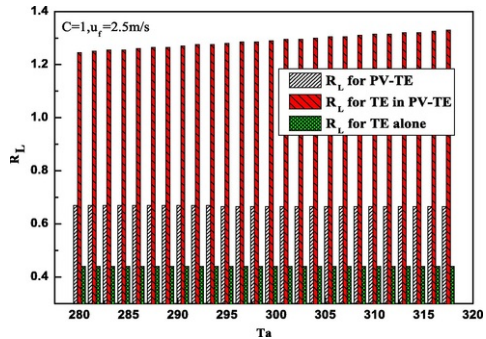
Fig. 6 Load resistances with different ambient temperature (based on c-Si).

4.2 PV-TE based on GaAs cell

It can be seen that for PV-TE module based on GaAs cell, the load resistance is also different from the one for the TE alone. From the Fig. 7, it can be indicated that the internal electrical resistance is about $2.0\,\Omega$. But when combined with the PV cell, the load resistance would be close to about $3.4\,\Omega$ for the TE maximum power output in the PV-TE. This is about 1.6 times than the internal resistance or the load resistance of the TE alone for the maximum output. And with the wind speed increase, the load resistance of the TE for TE maximum output in the PV-TE becomes slightly larger. However, for the PV-TE maximum power output, the internal resistance is lower than those for TE alone maximum power output, which is about just about $1.66\,\Omega$.
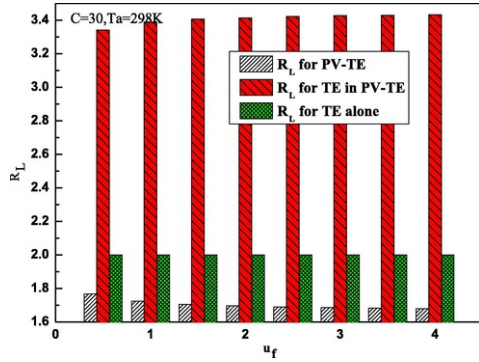
Fig. 7 Load resistances with different wind speeds (based on GaAs).

It is clear that for the GaAs cell, the high concentration ratio will enhance the PV temperature. As shown in Fig. 8, with the concentration ratio increase, the load resistance of TE for the maximum power output in the PV-TE module has a rising tendency. But for the PV-TE maximum power output, the value of the load resistance keeps a relative stable one. So in the PV-TE module, it is difficult to match the load resistance of TE for PV-TE maximum power output to refer to the value of the load resistance for TE maximum power output in PV-TE module.
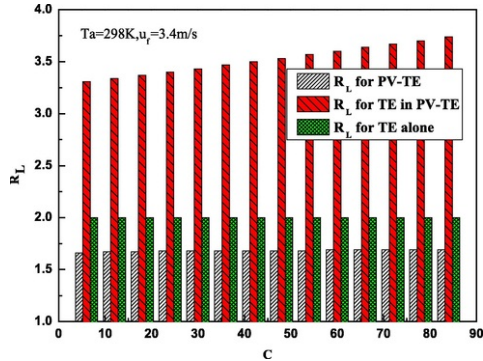
Fig. 8 Load resistances with different solar concentration ratios (based on GaAs).

The effect of the ambient temperature for the load resistance is clear, as shown in Fig. 9. With the ambient temperature increase, the load resistances for TE and PV-TE maximum power output in the PV-TE module have the opposite change trend. The load resistance for TE maximum power output in PV-TE module gradually becomes smaller, and the one for PV-TE maximum power output gradually becomes larger, which will be larger than the internal resistance of TE when the ambient temperature is higher than $310\,K$.
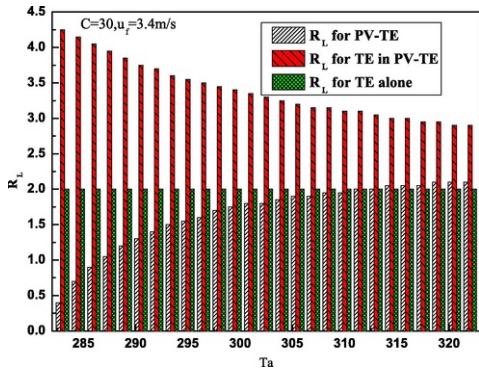
Fig. 9 Load resistances with different ambient temperature (based on GaAs).

From the analysis above it can be seen that the inconsistent phenomenon of TE load resistance is existent. The possible explanations may originate from the coupling effect between the PV and TE. The difference in load resistance may lead to the temperature difference of TE hot and cold sides since the difference in load resistance lead to the different current and further to the different electricity and heat percentages. Actually, when the load resistance is not equal to the internal resistance, the TE cannot produce the maximum output but provide the suitable temperature for PV then get the maximum output for the whole PV-TE module.

Therefore, the load resistance correlation for TE alone maximum output is unsuitable for determining the optimum load resistance for PV-TE module. In addition, in the test, if the load resistance is changed to meet the TE maximum power output, the load resistance is not equivalent to the one for PV-TE maximum power output, and the sum of the TE maximum power output and the PV power output under the same temperature condition is not the actual PV-TE module power output. In other words, when the load resistance matches the one for the PV-TE maximum power output, the output for TE does not correspond to the maximum output for TE alone or TE in the PV-TE module. Taking the PV-TE based on c-Si and GaAs for example, the data details are shown in Table 2. For the PV-TE based on c-Si, the internal resistance of TE is 0.47 Ω, and the load resistance of TE for TE maximum power output in the PV-TE is 1.40 Ω. But it is clearly that when the load resistance matches the TE maximum power output, whatever in the TE alone or in the PV-TE, the total PV-TE efficiency is lower than that with the load resistance of 0.75 Ω. The inconsistent phenomenon of TE also occurs in the PV-TE based on the GaAs cell. Thus, in the PV-TE, it is not always the optimize output when only depending on the internal resistance of TE or the load resistance responding to the TE maximum output to match the TE maximum power output.

Table 2 Details of different efficiencies with different load resistances.

	Load resistance of TE (Ω)	TE efficiency (%)	PV-TE efficiency (%)
Based on c-Si	0.47	1.30	11.04
	1.40	1.67	10.95
	0.75	1.57	11.07
Based on GaAs	2.00	1.01	22.90
	3.40	1.20	22.83
	1.60	1.03	22.94

5 Conclusion

In this paper, the inconsistent phenomenon of TE load resistance for photovoltaic–thermoelectric module was indicated. The model of the PV-TE was built and verified. The load resistances in different ambient conditions were also presented.

Due to the coupling effect of PV and TE, the characteristic of the load resistance was changed, and the inconsistent phenomenon of TE load resistance is significant. The load resistances of TE for the maximum power output of

the TE alone, TE in PV-TE and PV-TE in different ambient conditions were compared. Different types of PV cells and different ambient conditions all affect the load resistance of TE. But it can be concluded that the load resistance of the TE alone is different from the load resistance of TE in PV-TE module, so the internal resistance of TE cannot be as the reference to match the load resistance for PV-TE module.

In addition, the load resistance of TE for TE maximum power output is not the one for PV-TE maximum power output. In actual application, the PV efficiency and TE efficiency may be all considered to match the load resistance of TE. Only considering the TE efficiency to match the load resistance may not also lead to a highest PV-TE efficiency. This paper would provide a reference to match a suitable a load resistance for the PV-TE maximum power output.

Acknowledgment

References

[1] Guiqiang Li, Xudong Zhao and Jie Ji, Conceptual development of a novel photovoltaic-thermoelectric system and preliminary economic analysis, *Energy Convers Manage* **126**, 2016, 935–943.

[2] Guiqiang Li, Jie Ji, Gan Zhang, Wei He, Xiao Chen and Hongbing Chen, Performance analysis on a novel micro-channel heat pipe evacuated tube solar collector incorporated thermoelectric generation, *Int J Energy Res* **40**, 2016, 2117–2127.

[3] W.G.J.H.M. van Sark, Feasibility of photovoltaic – thermoelectric hybrid modules, *Appl Energy* **88**, 2011, 2785–2790.

[4] Ravita Lamba and S.C. Kaushik, Modeling and performance analysis of a concentrated photovoltaic–thermoelectric hybrid power generation system, *Energy Convers Manage* **115**, 2016, 288–298.

[5] Ning Wang, Li Han, Hongcai He, Nam-Hee Park and Kunihito Koumoto, A novel high-performance photovoltaic–thermoelectric hybrid device, *Energy Environ Sci* **4**, 2011, 3676–3679.

[6] R. Bjørk and K.K. Nielsen, The performance of a combined solar photovoltaic (PV) and thermoelectric generator (TEG) system, *Sol Energy* **120**, 2015, 187–194.

[7] Wei Pang, Yu Liu, Shiquan Gao and Xin Gao, Empirical study on thermal performance through separating impacts from a hybrid PV/TE system design integrating heat sink, *Int Commun Heat Mass Transfer* **60**, 2015, 9–12.

[8] Wei Zhu, Yuan Deng, Yao Wang, Shengfei Shen and Raza Gulfam, High-performance photovoltaic-thermoelectric hybrid powergeneration system with optimized thermal management, *Energy* **100**, 2016, 91–101.

[9] X. Zhang and K.T. Chau, An automotive thermoelectric–photovoltaic hybrid energy system using maximum power point tracking, *Energy Convers Manage* **52** (1), 2011, 641–647.

[10] X. Zhang and K.T. Chau, Design and implementation of a new thermoelectric–photovoltaic hybrid energy system for hybrid electric vehicles, *Electr Power Comp Syst* **39** (6), 2011, 511–525.

[11] Y.J. Zhang, J. Fang, C. He, H. Yan, Z.X. Wei and Y.F. Li, Integrated energy-harvesting system by combining the advantages of polymer solar cells and thermoelectric devices, *J Phys Chem C* **117**, 2013, 24685–24691.

[12] K.T. Park, S.M. Shin, A.S. Tazebay, H.D. Um, J.Y. Jung, S.W. Lee, et al., Lossless hybridization between photovoltaic and thermoelectric devices, *Sci Rep* **3**, 2013, 2123.

[13] Wei He, Gan Zhang, Guiqiang Li and Jie. Ji, Analysis and discussion on the impact of non-uniform input heat flux on thermoelectric generator array, *Energy Convers Manage* **98**, 2015, 268–274.

[14] Guiqiang Li, Gan Zhang, Wei. He, Jie Ji, Song Lv, Xiao Chen, et al., Performance analysis on a solar concentrating thermoelectric generator using the micro-channel heat pipe array, *Energy Convers Manage* **112**, 2016, 191–198.

[15] Guiqiang Li, Wei Feng, Yi Jin, Xiao Chen and Jie Ji, Discussion on the solar concentrating thermoelectric generation using micro-channel heat pipe array, *Heat Mass Transf* **53** (11), 2017, 3249–3256.

[16] Song Lv, Wei He, Dengyun Hu, Jian Zhu, Guiqiang Li, Hongbing Chen, et al., Study of different heat exchange technologies influence on the performance of thermoelectric generators, *Energy Convers Manage* **156**, 2018 167–177.

[17] Adham Makki, et al., Numerical investigation of heat pipe-based photovoltaic–thermoelectric generator (HP-PV/TEG) hybrid system, *Energy Convers Manage* **112**, 2016, 274–287.

[18] Song Lv, Wei He, Liping Wang, Guiqiang Li, Jie Ji, Hongbing Chen, et al., Design, fabrication and feasibility analysis of a thermo-electric wearable helmet, *Appl Therm Eng* **109**, 2016, 138–146.

[19] Guiqiang Li, Gang Pei, Jie Ji and Yuehong Su, Outdoor overall performance of a novel air-gap-lens-walled compound parabolic concentrator (ALCPC) incorporated with photovoltaic/thermal system, *Appl Energy* **144**, 2015, 214–223.

[20] Guiqiang Li, Xiao Chen and Yi Jin, Analysis of the primary constraint conditions of an efficient photovoltaic-thermoelectric hybrid system, *Energies* **10**, 2017, 20.

[21] T.L. Bergman, F.P. Incropera and A.S. Lavine, Fundamentals of heat and mass transfer, 2011, John Wiley & Sons.

[22] Y.Y. Wu, S.Y. Wu and L. Xiao, Performance analysis of photovoltaic-thermoelectric hybrid system with and without glass cover, *Energy Convers Manage* **93**, 2015, 151–159.

[23] T.H. Kil, S. Kim, D.H. Jeong, D.M. Geum, S. Lee, S.J. Jung, et al., A highly-efficient, concentrating-photovoltaic/thermoelectric hybrid generator, *Nano Energy* **37**, 2017, 242–247.

Highlights

- Migration phenomenon of TE load resistance for PV-TE was indicated.
- The model of the PV-TE was built and verified.
- PV-TE based on two types of PV cells were analyzed.
- The load resistances in different ambient conditions were compared.

Queries and Answers

Query: Your article is registered as a regular item and is being processed for inclusion in a regular issue of the journal. If this is NOT correct and your article belongs to a Special Issue/Collection please contact jaya.bhaskaran@elsevier.com immediately prior to returning your corrections.
Answer: Yes

Query: The author names have been tagged as given names and surnames (surnames are highlighted in teal color). Please confirm if they have been identified correctly.
Answer: Yes

Query: Please check the address for the corresponding author that has been added here, and correct if necessary.
Answer: yes

Query: The country names of the Grant Sponsors are provided below. Please check and correct if necessary. 'National Science Foundation of China' - 'China', 'Anhui Provincial Natural Science Foundation' - 'China'.
Answer: Yes.

Query: One or more sponsor names may have been edited to a standard format that enables better searching and identification of your article. Please check and correct if necessary.
Answer: yes